

Si(100) Surface Reconstruction: Spectroscopic Selection of a Structural Model

Joel A. Appelbaum, G. A. Baraff, and D. R. Hamann

Bell Laboratories, Murray Hill, New Jersey 07974

(Received 10 July 1975)

Two qualitatively different structural models are currently popular for the stable 2×1 superstructure characteristic of the Si(100) surface. We report the results of realistic self-consistent calculations of the electronic spectrum for both. Comparison with uv photoemission data clearly favors the pairing model over the vacancy model. Our results on surface Fermi-level pinning and bond saturation support this conclusion.

The existence of a wide variety of superlattice periodicities on semiconductor surfaces has long been known through low-energy electron-diffraction studies.¹ An understanding of the origin of these surface structural instabilities and of the relationship between them and the electronic properties of the surface represents a major theoretical challenge in surface physics. Complicating the problem greatly is the fact that the arrangement of atoms within the superlattice unit cell is not known, such determinations not being presently within the capabilities of low-energy electron diffraction for semiconductors.

In order to explore the physics of semiconductor reconstruction, we have performed realistic self-consistent calculations of the electronic structure of the Si(100) surface. This surface was selected because it offers a number of advantages as a test case. It exists only in the 2×1 reconstructed phase, whose structure is the simplest possible.^{2,3} By contrast, the unreconstructed phase of the Si(111) surface is stable at high temperatures,⁴ the complex 7×7 phase is stable at low temperatures,^{2,3} and a metastable 2×1 phase exists which is formed only by cleavage.^{2,3} (This latter phase is the only reconstructed one for which realistic studies of the electronic structure have been reported.⁵) The unreconstructed (100) surface would have two broken bonds per atom, a manifestly unstable situation. This strong chemical instability suggests a limited number of plausible structural models.

One structural model, proposed by Schlier and Farnsworth, consists of alternate rows of atoms moved towards each other to form pairs (or dimers), thereby rebonding half the broken surface bonds.³ Phillips recently introduced another model for the 2×1 structure in which alternating vacancies and atoms are located along surface rows, and double bonds are formed between atoms of the first and second layers.⁶ (This must be distinguished from Lander and Morrison's origi-

nal vacancy model for a longer-period superlattice,⁷ the existence of which is now doubted.⁸) These two models represent two very different approaches to lowering the bonding energy of the surface, and we calculated the electronic structure of both. For the pairing model, we used Levine's geometry with all bonds equal to the bulk bond length of 2.35 Å.⁹ For the vacancy model, we used a double-bond length of 2.13 Å, as given by Pauling's formula,¹⁰ between the first and second layers, and kept the second-layer atoms in their ideal positions. These calculations completely parallel preliminary calculations for the unreconstructed Si(100) surface which have already been reported,¹¹ utilizing a fully self-consistent pseudopotential and semi-infinite geometry.

Some key features of the electronic structure of both models can be visualized in terms of the broken-bond orbitals shown schematically in Fig. 1. For the pairing model, the states which we find approximate the following linear combinations (which transform as the indicated irreducible representations of the symmetry group of the surface, C_{2v} ¹²):

$$|\sigma b\rangle = \frac{1}{2}(|1\rangle - |2\rangle - |3\rangle + |4\rangle), \quad A_1,$$

$$|\sigma a\rangle = \frac{1}{2}(|1\rangle - |2\rangle + |3\rangle - |4\rangle), \quad B_1,$$

$$|\pi b\rangle = \frac{1}{2}(|1\rangle + |2\rangle + |3\rangle + |4\rangle), \quad A_1,$$

$$|\pi a\rangle = \frac{1}{2}(|1\rangle + |2\rangle - |3\rangle - |4\rangle), \quad B_1,$$

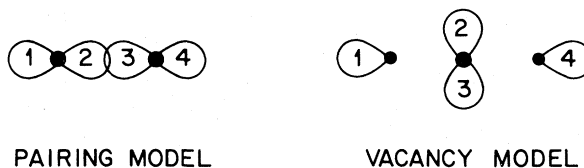


FIG. 1. Broken bonds for both surface models. All are directed up out of the page. Larger and smaller dots represent first- and second-layer atoms.

All the broken bonds can be regarded as "starting out" in the valence-conduction band gap. The "sigma bonding" combination $|\sigma b\rangle$ has its charge predominantly in the dimer region and is pulled down greatly by the pair-bond potential. It forms resonances and surface states among the valence bands. The corresponding antibonding state $|\sigma a\rangle$ has its charge in the region between the dimers and is pushed up into the conduction bands. The π -like bonding and antibonding states, derived from the dangling bonds of the ideal surface,¹¹ are split but remain in the gap. Their spectra are shown in Fig. 2. The surface Fermi level shown was determined by putting two electrons in these bands. It has been experimentally located at 0.2 ± 0.2 eV,¹³ which is consistent with our result for the pairing model. We expect the extra bonding contributed by $|\pi b\rangle$ to shorten the pair bond slightly from the assumed single-bond length. This would further separate the $|\pi a\rangle$ and $|\pi b\rangle$ bands to give a semiconducting surface instead of the slightly semimetallic surface presently found. A chemisorbed monolayer could form a single bond with each surface atom utilizing only π states. While this would remove the extra bonding, it would not affect the principal $|\sigma b\rangle$ bond, and thus not disturb the paired structure.¹¹

To discuss the vacancy model, consider its broken bonds shown in Fig. 1 combined in the symmetry orbitals

$$|\pi b\rangle = \frac{1}{2}(|1\rangle + |2\rangle + |3\rangle + |4\rangle), \quad A_1,$$

$$|\pi a\rangle = \frac{1}{2}(|1\rangle - |2\rangle - |3\rangle + |4\rangle), \quad A_1,$$

$$|1\text{ br}\rangle = \frac{1}{2}\sqrt{2}(|2\rangle - |3\rangle), \quad B_2,$$

$$|2\text{ br}\rangle = \frac{1}{2}\sqrt{2}(|1\rangle - |4\rangle), \quad B_1.$$

These states remain almost completely in the gap. The flat π bonding and antibonding bands are split by 1.5 to 2 eV (see Fig. 2). They are overlapped by broad bands of nonbonding states whose charge is located in first- and second-layer bridge positions, $|1\text{ br}\rangle$ and $|2\text{ br}\rangle$. These are similar to states found for the unreconstructed surface.¹¹ Distributing four electrons among these bands partially fills the bridge bands and leaves the Fermi level pinned at midgap.

Since only one filled π bonding band exists and there are two bonds in the surface unit cell, we conclude that the double bonding invoked in support of this model is not achieved. An unstable metallic surface remains, and we infer from the nature of the states involved that readjustments of the atomic positions will not qualitatively

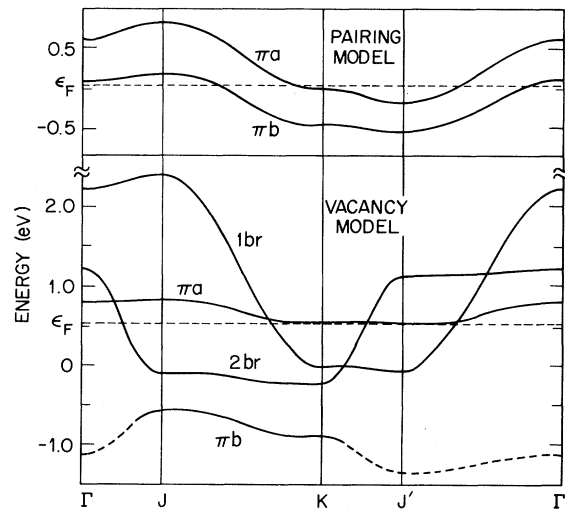


FIG. 2. Dispersion relations for surface states near the absolute gap. Energy is measured from the valence-band maximum, and surface Brillouin-zone symmetry points are defined in Ref. 11. Dashed curves are resonances, and the hybridization gaps at symmetry-forbidden crossings are omitted for clarity.

change this situation.

The densities of occupied states in the surface regions (including 2 and 2.5 atomic layers for the pairing and vacancy models, respectively) were calculated based on a sampling of 700 surface and scattering states. The sample points were smoothed with the Gaussian $\exp(-3.4\epsilon^2)$, and we verified good convergence of the density of states using this sample smoothing. The results from both models are compared to the photoemission spectrum at $\hbar\omega = 21.2$ eV¹⁴ in Fig. 3. A smooth background of estimated secondaries has been subtracted from the data, and the curves are aligned on the basis of surface Fermi energy. We believe that the device of calculating the density of states spatially integrated over the first few atomic layers gives a reasonable approximation to the escape-depth weighting operative in the 21-eV photon-energy range.

The most immediately apparent difference between the data and either theoretical density of states is the strong suppression of emission from the s -band region (below -8 eV). This is common to all surfaces, and is presumably a matrix-element effect. Major differences in the spectrum of the (100) surface from the others studied in Ref. 14 show up primarily in the p -band region, 0 to -5 eV. Most distinctive are the rapid rise in emission below threshold, the symmetric

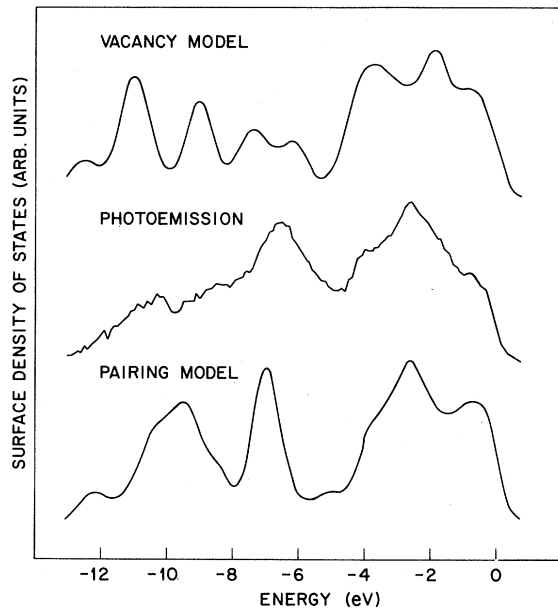


FIG. 3. Calculated surface-region density of states compared to $\hbar\omega = 21.2$ -eV photoelectron-energy distribution from Ref. 13, with estimated secondaries subtracted.

triangular peak at -2.5 eV, and the shoulder at -4 eV. These are fitted much better by the pairing model than by the vacancy model. The peak at -7 eV, while not a unique feature of the (100) surface, is well reproduced by the pairing model, but split by the vacancy model. We believe that this comparison constitutes substantial evidence that the pairing geometry is, within minor refinements, the correct one.

To identify the physical origin of features in the spectrum of the pairing model, we examined the density of states at several individual points within the surface region. The surface enhancement in the range 0 to -1 eV is due to spectral weight from the broken bonds pulled down by the formation of the $|\pi b\rangle$ band, and weight in the backbonds pushed up by the bending distortion. The bulklike peak at -7 eV also gets a large contribution from the backbond and is 0.3 eV higher than the bulk peak given by our pseudopotential. The spectrum at the pair bond is highly peaked at -2.5 and -9.5 eV, quite unlike the bulk case. The total charge density in the pair bond is shown in Fig. 4, and is very similar to a bulk bond in the closed-contour region. We believe that its spectrum is so different because angular misalignment keeps it from hybridizing strongly with neighboring bonds.

In conclusion, we have demonstrated that elec-

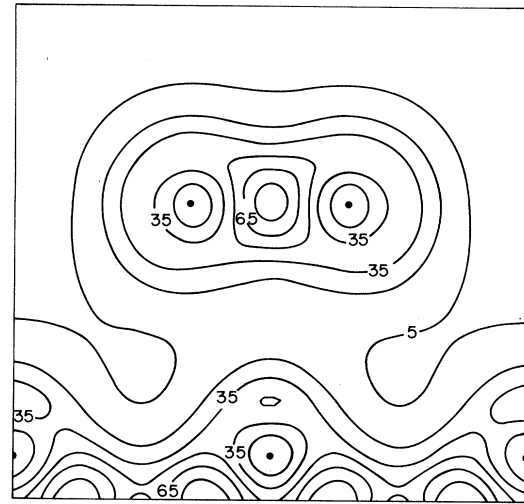


FIG. 4. Charge-density contours on a plane normal to the surface passing through the paired surface atoms and fourth-layer atoms (shown by dots). Second- and third-layer atoms lie out of this plane. Density is in atomic units $\times 10^{-3}$.

tronic-structure calculations, in combination with spectroscopic data, can draw meaningful distinctions among structural models for semiconductor reconstruction, and can elucidate the physical mechanisms underlying these phenomena.

We wish to thank J. E. Rowe for helpful discussions and for providing the data in Fig. 3.

¹J. J. Lander, *Prog. Solid State Chem.*, **2**, 26 (1965).

²R. E. Schlier and H. E. Farnsworth, *J. Chem. Phys.*, **30**, 917 (1959). In this and other early low-energy electron-diffraction studies, the authors describe the Si(100) pattern as 2×2 , yet recognize that it is really a superposition of the two possible domains of the 2×1 structure.

³D. Haneman, *Phys. Rev.*, **121**, 1093 (1961); F. Jona, *IBM J. Res. Dev.*, **9**, 375 (1965).

⁴J. E. Florio and W. D. Robertson, *Surf. Sci.*, **24**, 17 (1971).

⁵K. C. Pandey and J. C. Phillips, *Phys. Rev. Lett.*, **34**, 1450 (1975); M. Schlüter *et al.*, *Phys. Rev. Lett.*, **34**, 1385 (1975).

⁶J. C. Phillips, *Surf. Sci.*, **40**, 459 (1973).

⁷J. J. Lander and J. Morrison, *J. Chem. Phys.*, **30**, 917 (1959). These authors observed fourth-order diffraction features, and proposed a structural model with $\sqrt{2} \times 2\sqrt{2}$, or "centered 2×4 ," periodicity. A complete

layer was assumed to form pairs, and an additional paired half layer to bond to the remaining free bonds of the complete paired layer. Only single bonds were considered. The same local bonding arrangement could also produce a 2×2 structure, but not a 2×1 .

⁸P. M. Gundry *et al.*, *Surf. Sci.*, **43**, 651 (1974). These authors showed that fourth-order features produced by high-temperature annealing like that used by Lander and Morrison may be due to the formation of (111) facets.

⁹J. Levine, *Surf. Sci.*, **34**, 90 (1973).

¹⁰L. Pauling, *The Nature of the Chemical Bond* (Cornell Univ. Press, Ithaca, N.Y., 1960), 3rd ed., p. 239.

¹¹J. A. Appelbaum, G. A. Baraff, and D. R. Hamann, *Phys. Rev. B* **11**, 3822 (1975), and to be published.

¹²M. Hamermesh, *Group Theory* (Addison-Wesley, Reading, Mass., 1962), p. 125.

¹³J. E. Rowe, *Phys. Lett.*, **46A**, 400 (1974).

¹⁴J. E. Rowe and H. Ibach, *Phys. Rev. Lett.*, **32**, 421 (1974).

Measurement of Equilibrium Critical Velocities for Vortex Formation in Superfluid Helium*

Keith DeConde and Richard E. Packard

Physics Department, University of California, Berkeley, California 94720

(Received 10 July 1975)

We have made measurements of the critical velocity for vortex formation in right cylinders of circular, elliptical, and rectangular cross section. The procedure used seems to produce the superfluid in its equilibrium state and the results are in good quantitative agreement with theoretical calculations based on equilibrium thermodynamics.

Since the predictions of Onsager and Feynman it has been widely demonstrated that quantized vorticity can exist in superfluids. Quantized vortex lines provide striking evidence for the fundamentally quantum nature of a superfluid, and the creation of quantized vortices apparently is the process which limits "super" or dissipationless flow of superfluids to small velocities. For these reasons the study of critical velocities for vortex creation is of significant theoretical and experimental interest.¹ This paper presents reproducible measurements of the critical velocity which are in quantitative agreement with theoretical calculations made by Fetter.²

The critical velocity Ω is generally difficult to calculate because of complicated geometries and it is difficult to measure because of the irreproducible metastability which is characteristic of flowing He II.³ The most rigorous calculations performed up to now are those which treat vortex lines in rotating cylinders.⁴ These calculations, which are based on equilibrium thermodynamics, predict the minimum angular velocity, Ω_c , at which the free energy will be minimized by the presence of one vortex line. Recently calculations have included cylinders without rotational symmetry,² although no quantitative experimental verification has been available. The main disparity between the free-energy calculations and actual measurements of critical velocities is that in most experimental situations the flowing He II exists in a metastable state rather than the

equilibrium state. This metastability exists because of large energy barriers between flow states which are themselves local minima in the free energy.

For example, consider a circularly cylindrical bucket containing one quantized vortex in the center, and rotating with an angular velocity at which the equilibrium state would have no vortices. If the system passes to the equilibrium state via simple translation of the line to the wall, it requires an energy of $\sim 10^9$ K! Thus, as the vessel slows down the line may persist to speeds well below Ω_c , the critical velocity predicted from the equilibrium theory.

We have found a process which seems to put a sample of rotating He II into a true equilibrium state thus enabling us to verify quantitatively some of the equilibrium predictions of critical velocities. The basic process has been used previously by others⁵ and simply consists of initially rotating the liquid above the λ point until internal mechanical equilibrium exists and then subsequently cooling the steadily rotating sample to below T_λ .

There are several reasons for expecting this process to yield the equilibrium state. The most likely explanation is that the energy barriers become vanishingly small near T_λ because they are proportional to the superfluid density ρ_s . If transitions between different flow states are thermally activated or are caused by random apparatus vibrations, equilibrium should be reached rapid-